Cancer Letters 446 (2019) 90–102

Contents lists available at ScienceDirect

Cancer Letters

journal homepage: www.elsevier.com/locate/canlet

Original Articles

New inhibitor of the TAp73 interaction with MDM2 and mutant p53 with promising antitumor activity against neuroblastoma

Sara Gomes[a,1], Liliana Raimundo[a,1], Joana Soares[a,1], Joana B. Loureiro[a], Mariana Leão[a], Helena Ramos[a], Madalena N. Monteiro[a], Agostinho Lemos[b], Joana Moreira[b], Madalena Pinto[b], Petr Chlapek[c,d], Renata Veselska[c,d], Emília Sousa[b,**], Lucília Saraiva[a,*]

[a] LAQV/REQUIMTE, Laboratório de Microbiologia, Departamento de Ciências Biológicas, Faculdade de Farmácia, Universidade do Porto, Rua de Jorge Viterbo Ferreira n.° 228, 4050-313, Porto, Portugal

[b] CIIMAR, Laboratório de Química Orgânica e Farmacêutica, Departamento de Ciências Químicas, Faculdade de Farmácia, Universidade do Porto, Rua de Jorge Viterbo Ferreira n.° 228, 4050-313, Porto, Portugal

[c] Laboratory of Tumor Biology, Department of Experimental Biology, Faculty of Science, Masaryk University, 61137, Brno, Czech Republic

[d] International Clinical Research Center, St. Anne's University Hospital, 65691, Brno, Czech Republic

ARTICLE INFO

Keywords:
p73
Carbaldehydic xanthone
Anticancer therapy

ABSTRACT

TAp73 is a key tumor suppressor protein, regulating the transcription of unique and shared p53 target genes with crucial roles in tumorigenesis and therapeutic response. As such, in tumors with impaired p53 signaling, like neuroblastoma, TAp73 activation represents an encouraging strategy, alternative to p53 activation, to suppress tumor growth and chemoresistance.

In this work, we report a new TAp73-activating agent, the 1-carbaldehyde-3,4-dimethoxyxanthone (LEM2), with potent antitumor activity. Notably, LEM2 was able to release TAp73 from its interaction with both MDM2 and mutant p53, enhancing TAp73 transcriptional activity, cell cycle arrest, and apoptosis in p53-null and mutant p53-expressing tumor cells. Importantly, LEM2 displayed potent antitumor activity against patient-derived neuroblastoma cells, consistent with an activation of the TAp73 pathway. Additionally, potent synergistic effects were obtained for the combination of LEM2 with doxorubicin and cisplatin in patient-derived neuroblastoma cells. Collectively, besides its relevant contribution to the advance of TAp73 pharmacology, LEM2 may pave the way to improved therapeutic alternatives against neuroblastoma.

1. Introduction

p53 family proteins have a highly conserved gene structure including an N-terminal transactivation domain (TAD), a central DNA-binding domain (DBD), and a C-terminal oligomerization domain [1]. The *TP63* and *TP73* genes generate oncogenic transcriptionally inactive ΔN isoforms, lacking the TAD, and tumor suppressive TA isoforms, which retain an intact TAD [2]. Additionally, several TA and ΔN isoforms (e.g. α, β, and γ) are produced through C-terminal alternative splicing [2–4]. TAp73 regulates unique or shared p53 target genes involved in key cellular processes such as proliferation, cell cycle, apoptosis, and metastasis [5,6]. TAp73 also plays a crucial role in chemotherapy response. In fact, TAp73 is induced by chemotherapeutics like taxol, etoposide, cisplatin, and doxorubicin (DOXO), and its functional impairment enhances chemoresistance [7]. Unlike p53, p73 is rarely mutated in human cancers [8]. However, TAp73, particularly TAp73α, is often inactivated through interaction with mutant p53 (mutp53) and MDM2. In fact, one of the oncogenic mutp53 gain-of-function mechanisms occurs through interaction with TAp73, blocking its transcriptional activity, decreasing its ability to trigger apoptosis [5,9–11], and promoting invasion [12]. Likewise, MDM2, the major negative regulator of p53, binds to TAp73 blocking its transcriptional

Abbreviations: CETSA, cellular thermal shift assay; CFU, colony-forming unit; CI, combination index; Co-IP, co-immunoprecipitation; DOXO, doxorubicin; DRI, dose reduction index; ETOP, etoposide; MDM, murine double minute; MTT, 3-[4,5-dimethylthiazol-2-yl]-2,5-diphenyltetrazolium bromide; mut, mutant; NBL, neuroblastoma; SRB, sulforhodamine B; wt, wild-type; VEGF, vascular endothelial growth factor

* Corresponding author.
** Corresponding author.
E-mail addresses: esousa@ff.up.pt (E. Sousa), lucilia.saraiva@ff.up.pt (L. Saraiva).

[1] Authors contributed equally to this work.

https://doi.org/10.1016/j.canlet.2019.01.014
Received 27 September 2018; Received in revised form 19 December 2018; Accepted 9 January 2019

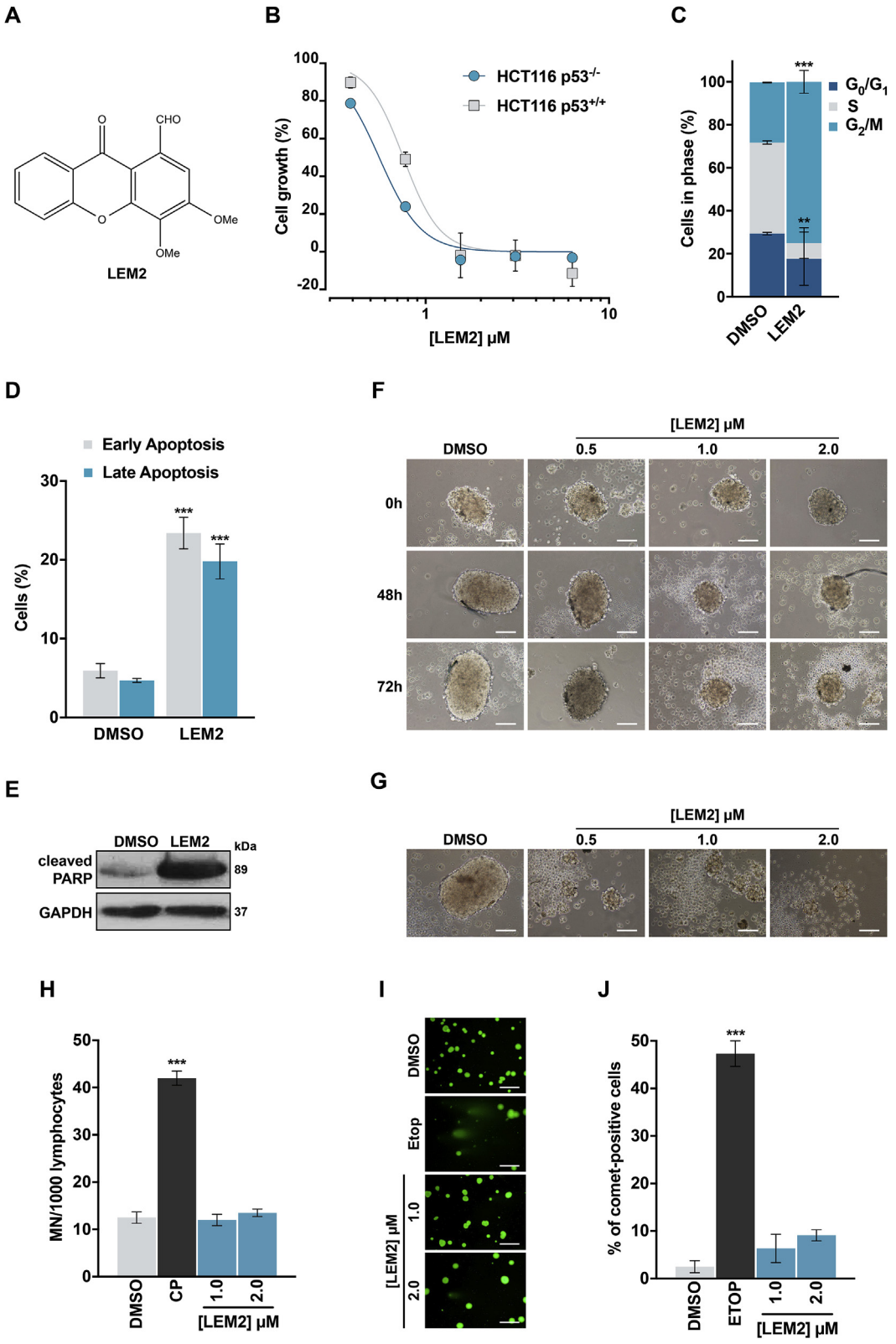

(caption on next page)

activity [13–16].

In p53-impaired tumors, TAp73 activation may compensate for the lack of a functional p53 pathway, suppressing tumor proliferation and increasing chemotherapeutic efficiency [17]. In these tumors, disruption of the TAp73 interaction with mutp53 and MDM2 represents an encouraging therapeutic strategy, alternative to p53 activation. Consistently, the MDM2-inhibitor nutlin-3a [18] was reported to suppress cell growth in p53-null tumor cells through inhibition of the TAp73α-MDM2 interaction [19]. Additionally, SIMPs (short interfering mutp53 peptides) were shown to activate TAp73α through disruption of the mutp53-TAp73α interaction, sensitizing mutp53-expressing cells to adriamycin and cisplatin [20]. More recently, RETRA [21], prodigiosin

Fig. 1. LEM2 is a non-genotoxic drug with p53-and p63-independent growth inhibitory activity in human tumor cells. (A) Chemical structure of LEM2. (B) Dose-response curves for the growth inhibitory activity of 0.39–6.25 μM LEM2 in $p53^{+/+}$ and $p53^{-/-}$ HCT116 cells, determined by SRB assay, after 48 h treatment. Data are mean ± SEM (n = 4). (C) Effect of 2 μM LEM2 on cell cycle progression of HCT116 $p53^{-/-}$ cells after 24 h treatment. Data are mean ± SEM (n = 3); values significantly different from DMSO: $^{**}p < 0.01$, $^{***}p < 0.001$ (two-way ANOVA with Dunnett's multiple comparison test). (D) Effect of 2 μM LEM2 on apoptosis of HCT116 $p53^{-/-}$ cells after 48 h treatment. Data are mean ± SEM (n = 4); values significantly different from DMSO: $^{***}p < 0.001$ (one-way ANOVA with Dunnett's multiple comparison test). (E) Levels of cleaved PARP in HCT116 $p53^{-/-}$ cells after 48 h treatment with 1 μM LEM2 or solvent, visualized by western blot. Immunoblots represent one of three independent experiments; GAPDH was used as a loading control. (F) Brightfield imaging of 3-day-old HCT116 $p53^{-/-}$ spheroids, treated with LEM2 or solvent for 48 and 72 h. (G) Brightfield imaging of HCT116 $p53^{-/-}$ spheroids formed after 7 days. Spheroids were seeded in the presence of LEM2 or solvent. In F and G, images are representative of 3 independent experiments; scale bar = 100 μm; magnification = 100×. (H) Analysis of the genotoxicity in human lymphocytes measured by cytokinesis-block micronucleus assay, following 72 h treatment with 5 μg/mL cyclophosphamide (CP; positive control), or LEM2 (n = 3); values significantly different from DMSO: $^{***}p < 0.001$ (one-way ANOVA with Dunnett's multiple comparison test). (I,J) DNA damage was measured in HCT116 $p53^{-/-}$cells by comet assay after 48 h treatment with 50 μM etoposide (ETOP; positive control) or LEM2. In I, representative images of the comet assay (scale bar = 50 μm; magnification = 100×). In J, quantification of comet-positive cells (containing more than 5% of DNA in the tail); one hundred cells were analyzed in each group (n = 3); values significantly different from DMSO: $^{***}p < 0.001$ (one-way ANOVA with Dunnett's multiple comparison test).

[22], and benzyl isothiocyanate [23] have also been reported as mutp53-TAp73α interaction inhibitors with antitumor activity.

Neuroblastoma (NBL) is one of the most common childhood solid cancers [24]. Even with the currently available therapeutic options, high-risk patients still have low survival rates [25]. In NBL, p53 is commonly sequestered in the cytoplasm, but TAp73α retains normal nuclear location [26]. Additionally, ΔNp73 overexpression is frequent in NBL, correlating with tumor progression and poor prognosis [27]. MDM2 amplification has also been reported in NBL [28], and although p53 mutations are rare in primary NBL [29], they have been reported as a mechanism of therapeutic resistance in relapsed tumors [30]. Therefore, the TAp73-activating strategies referred above arise as promising therapeutic approaches against NBL [31], particularly in combination with other therapies to potentiate their antitumor effect. In fact, nutlin-3a-induced TAp73α activation was shown to sensitize chemoresistant p53-null NBL cells to DOXO [32].

Herein, we report the identification of 1-carbaldehyde-3,4-dimethoxyxanthone (LEM2), a new activator of TAp73 by disrupting its interaction with both MDM2 and mutp53. LEM2 reveals promising antitumor activity, alone and in combination therapy, particularly against patient-derived NBL cells.

2. Materials and methods

2.1. Compounds

LEM2 synthesis is described in Supplementary Materials and Fig. S1. Etoposide, DOXO, nutlin-3a, cyclophosphamide (Sigma-Aldrich, Portugal), and LEM2 were dissolved in DMSO (Sigma-Aldrich). Cisplatin (Enzo Life Sciences, Taper, Portugal) was dissolved in saline.

2.2. Human cell lines and growth conditions

Colon adenocarcinoma HCT116 cells (HCT116 $p53^{+/+}$) and its p53-null isogenic derivative (HCT116 $p53^{-/-}$) were provided by Dr. Vogelstein (The Johns Hopkins Kimmel Cancer Center, Baltimore, USA); breast adenocarcinoma SK-BR-3, MDA-MB-231, MDA-MB-468, rectal adenocarcinoma SW-837, colorectal adenocarcinoma HT-29, and neuroblastoma SH-SY5Y cells were from ATCC (Rockville, MD, USA); hepatocellular carcinoma HuH-7 cells were from JCRB Cell Bank (Osaka, Japan). Cells were cultured in RPMI-1640 with UltraGlutamine (Lonza, VWR, Portugal) with 10% FBS (Gibco, Alfagene, Portugal), at 37 °C with 5% CO_2. SH-SY5Y cells were cultured in DMEM/F-12 (Lonza) with 10% FBS and 2 mM L-glutamine (Gibco).

2.3. Patient-derived NBL cells

Five patient-derived NBL cell lines (NBL-12, NBL-14, NBL-28, NBL-38, NBL-40) were established from tumor tissue samples as described [33,34], with written informed consent obtained for our previous research project (IGA MZCR NR/9125-4), approved by the Research Ethics Committee of the School of Medicine, Masaryk University, Brno, Czech Republic (Approval No. 23/2005). According to Czech legal and ethical regulations governing the use of human biological material for research purposes, a new ethical assessment of this study is not necessary.

Tumors were histologically characterized according to WHO classification. Cells were cultured in DMEM, with 20% fetal calf serum, 2 mM L-glutamine, 100 IU/mL penicillin, and 100 μg/mL streptomycin (all from Biosera, France), at 37 °C with 5% CO_2.

2.4. Cell proliferation and viability assays

For sulforhodamine B (SRB) assay: cells were seeded in 96-well plates at 5.0×10^3 (HCT116, parental and transfected HT-29, HuH-7, SW-837), 7.5×10^3 (SK-BR-3, MDA-MB-468), and 1.0×10^4 (MDA-MB-231) cells/well, and IC_{50} values of compounds were determined as described [35].

For MTT assay: cells were seeded in 96-well plates at 7.5×10^3 (SH-SY5Y), 4.0×10^3 (NBL-12), 5×10^3 (NBL-14, NBL-38, NBL-40), and 6.0×10^3 (NBL-28) cells/well and IC_{50} values of compounds were determined as described [35,36].

For colony formation assay: MDA-MB-468 and transfected HCT116 $p53^{-/-}$ cells were seeded in 6-well plates at 5.0×10^2 cells/well, followed by 24 h incubation with LEM2 or solvent. Colonies were grown for 10 days in compound-free medium, fixed, stained and analyzed as described [37].

2.5. Transfection of p73 siRNA and ectopic expression of TAp73α

HCT116 $p53^{-/-}$ cells were transfected with 100 nM siRNAs against p73 (SMARTpool p73) and nonspecific siRNAs (Non-targeting Pool) from Thermo Scientific/Dharmacon (Portugal), using Lipofectamine 2000 (Invitrogen, Alfagene), according to manufacturer's instructions.

Transfection of HT-29 cells with a pCI-neo-TAp73α plasmid or the empty vector was performed with the ScreenFectA reagent (NZYTech, Portugal).

2.6. Cell cycle and apoptosis

Immortalized cells were seeded in 6-well plates at 1.5×10^5 (HCT116 $p53^{-/-}$) and 2.25×10^5 (MDA-MB-468, SH-SY5Y) cells/well, and patient-derived NBL cells in ⌀100 mm petri dishes at 4×10^5 cells/dish, followed by treatment with LEM2 or solvent. Cell cycle and apoptosis were analyzed as described [38]. The Accuri™ C6 flow cytometer and the BD Accuri C6 software (BD Biosciences) were used. For patient-derived NBL cells, the BD FACSVerse™ flow cytometer with BD FACSuite software (Beckton Dickinson, USA) were used. Cell cycle phases were quantified using FlowJoX 10.0.7 (Treestar, USA).

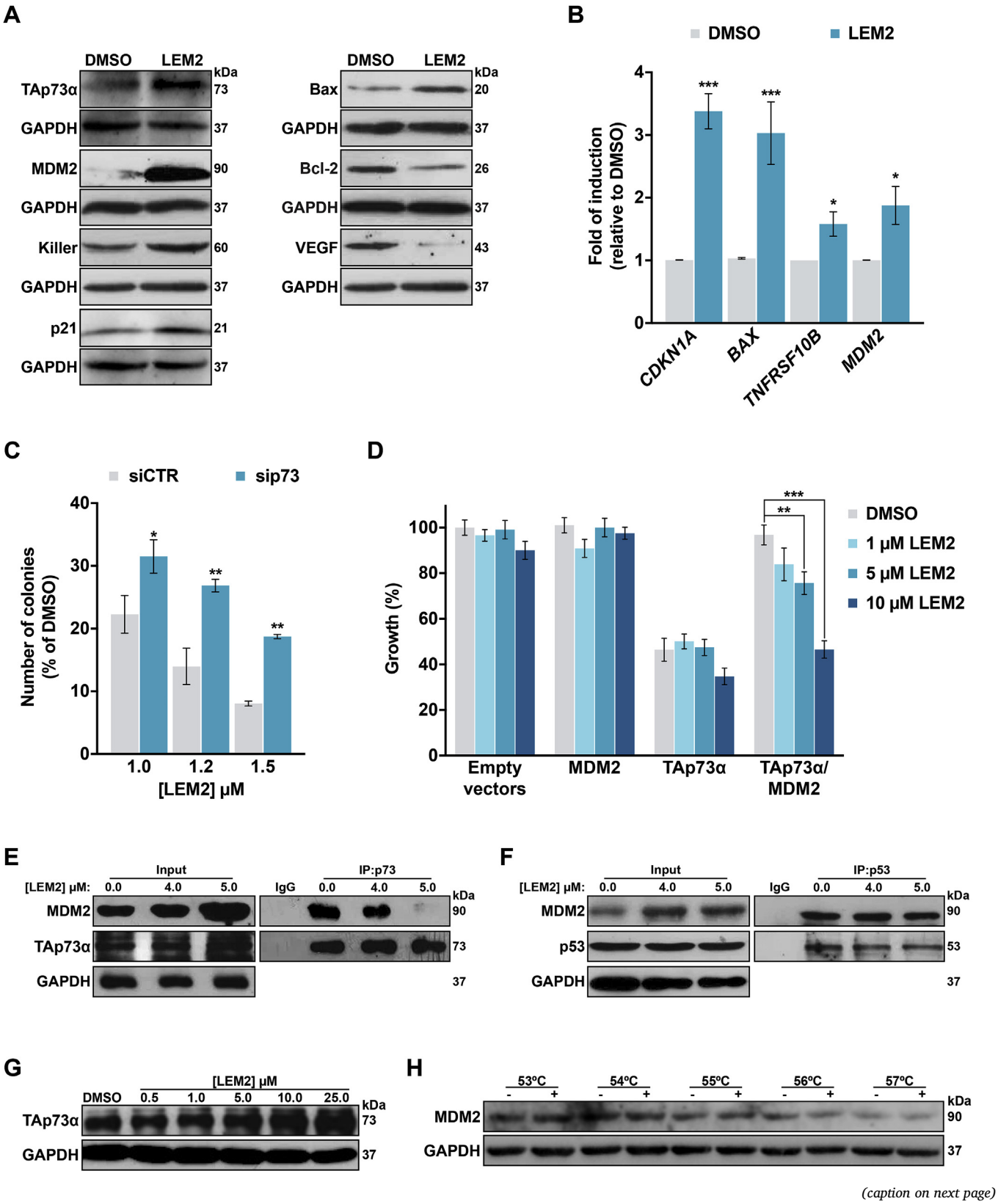

(caption on next page)

2.7. Generation of colon cancer spheroids

HCT116 p53$^{-/-}$ cells were seeded in 24-well plates at 1×10^3 cells/well in DMEM/F12 medium supplemented as described [37], with LEM2 or solvent; spheroids were grown for 7 days. Alternatively, colonospheres were grown in compound-free medium for 3 days, followed by LEM2 or solvent treatment for 3 days [39].

2.8. RNA extraction and RT-qPCR

Imortalized cells were seeded in 6-well plates at 1.5×10^5 (HCT116 p53$^{-/-}$) or 2.25×10^5 (MDA-MB-468) cells/well, and patient-derived

Fig. 2. LEM2 has TAp73-dependent growth inhibitory activity in human tumor cells, activating TAp73 through disruption of its interaction with MDM2 and inducing TAp73 thermal stabilization. (A) Protein levels of TAp73 transcriptional targets in HCT116 $p53^{-/-}$ cells, after 16 h (p21 and Bax) 24 h (MDM2, Killer, Bcl-2, VEGF) or 48 h (TAp73α) treatment with 1 μM LEM2 or solvent, visualized by western blot. (B) mRNA levels of TAp73 transcriptional targets measured by RT-qPCR in HCT116 $p53^{-/-}$ cells after 24 h treatment with 2 μM LEM2 or solvent. Fold of induction is relative to solvent. Data are mean ± SEM (n = 3); values significantly different from solvent: $*p < 0.05$, $***p < 0.001$ (two-way ANOVA with Dunnett's multiple comparison test). (C) Effect of LEM2 on the colony formation of HCT116 $p53^{-/-}$ cells transfected with siRNA targeting p73 (sip73) or control siRNA (siCTR). Cells were treated with LEM2 or solvent for 24 h, and colonies were allowed to grow for 10 days. Data are mean ± SEM (n = 3); values significantly different from siCTR: $*p < 0.05$, $**p < 0.01$ (two-way ANOVA with Sidak's multiple comparison test). (D) Effect of LEM2 on the growth of control yeast (empty vectors), yeast expressing TAp73α alone, and yeast co-expressing TAp73α and MDM2, after 40 h treatment. Results were plotted setting the growth of untreated control yeast as 100%; data are mean ± SEM (n = 4); values significantly different from DMSO: $**p < 0.01$, $***p < 0.001$ (two-way ANOVA with Dunnett's multiple comparison test). (E) Co-immunoprecipitation in HCT116 $p53^{-/-}$ cells treated with 4 and 5 μM LEM2 or solvent for 24 h, using anti-immunoglobulin G (IgG) or anti-TAp73α (IP:p73) antibodies followed by immunoblotting with anti-MDM2. (F) Co-immunoprecipitation in HCT116 $p53^{+/+}$ cells treated with 4 and 5 μM LEM2 or solvent for 24 h, using anti-immunoglobulin G (IgG) or anti-p53 (IP:p53) antibodies followed by immunoblotting with anti-MDM2. (G,H) CETSA in HCT116 $p53^{-/-}$ cell lysates treated with LEM2 or solvent; soluble protein was analyzed by western blot. In G, lysate samples were treated with 0.5–25 μM LEM2 and heated at 56 °C. In H, lysate samples were treated with 25 μM LEM2 (+) or solvent (−) and heated at increasing temperatures. In A, and E-H, immunoblots represent one of three independent experiments; GAPDH was used as a loading control.

NBL cells in ⌀100 mm petri dishes at 4×10^5 cells/dish, followed by treatment with LEM2 or solvent.

Immortalized cells: total RNA was extracted using Illustra™ RNAspin Mini RNA Isolation Kit (GE Healthcare, VWR); RT-qPCR was performed as described [39].

Patient-derived NBL cells: total RNA was extracted using GenElute™ Mammalian Total RNA Miniprep Kit (Sigma-Aldrich, Germany); RT-qPCR was performed as described [36]. Primer sequences are listed in Supplementary Table S1.

2.9. Western blot

Immortalized cells were seeded in 6-well plates at 1.5×10^5 (HCT116 $p53^{-/-}$) or 2.25×10^5 (MDA-MB-468) cells/well, and patient-derived NBL cells in ⌀100 mm petri dishes at 4×10^5 cells/dish, followed by treatment with LEM2 or solvent. Protein fractions were analyzed as described [40]. For yeast, western blot was performed as described [41]. Antibodies are listed in Supplementary Table S2.

2.10. Yeast transformation, growth and screening assay

Saccharomyces cerevisiae cells expressing human TAp73α alone or co-expressed with human MDM2 were used, as described [42]. Yeast expressing human TAp73α and/or mutp53-R273H were obtained using pRS314-(*TRP1*)-*GAL1-10*-TAp73α and pLS76-(*LEU2*)-*ADH1*-mutp53-R273H, and respective empty vectors by the LiAc/SS Carrier DNA/PEG method [43]. Yeast screening assay was performed by measuring the growth of yeast cells in selective galactose medium, as described [42]. Briefly, the expression of TAp73α in yeast induces growth arrest, which is abolished by co-expression of MDM2/mutp53; potential inhibitors of the TAp73α-MDM2/mutp53 interactions should restore the TAp73α-induced yeast growth arrest while not interfering with the growth of control yeast (empty vectors) and yeast expressing TAp73α, MDM2, or mutp53 alone.

2.11. Co-immunoprecipitation (co-IP)

Co-IP was performed using the Pierce Classic Magnetic IP and Co-IP Kit (Thermo Scientific, Dagma, Portugal), according to manufacturer's instructions [44]. p53, TAp73α, MDM2 and GAPDH were detected by western blot.

2.12. Cellular thermal shift assay (CETSA)

To evaluate drug target interactions in cells, the CETSA analysis was performed, as described [44,45]. Briefly, the impact of LEM2 on TAp73α/MDM2/mutp53 thermal stabilization was evaluated by assessing the amount of soluble protein (upon heating of tumor cell lysates) by western blot; after heating, whereas unbound (non-stabilized) proteins denature and precipitate, ligand-bound (stabilized) proteins remain in solution.

2.13. Comet assay

DNA damage was evaluated in HCT116 $p53^{-/-}$ cells, as described [39]. Cells containing more than 5% of DNA in the tail (assessed using OpenComet/ImageJ [46,47]) were considered comet positive.

2.14. Micronucleus assay

Cytokinesis-block micronucleus assay in human lymphocytes was performed as described [44].

2.15. Combination therapy assay

SH-SY5Y and patient-derived NBL-14 cells were treated with a fixed LEM2 concentration, and increasing concentrations of DOXO/cisplatin. Cell viability was analyzed by MTT assay. Combination index (CI) and dose reduction index (DRI) values were determined as described [39,48].

2.16. Statistical analysis

Data were statistically analyzed using GraphPad Prism. Different statistical tests were used depending on dataset; p values < 0.05 were considered statistically significant.

3. Results

3.1. LEM2 is a non-genotoxic drug with p53-independent growth inhibitory activity in human tumor cells

The antitumor activity of LEM2 (Fig. 1A) was evaluated in human wtp53-expressing HCT116 $p53^{+/+}$ and respective p53-null isogenic derivative HCT116 $p53^{-/-}$ cells, by SRB assay (Fig. 1B). The results showed that LEM2 had potent p53-independent tumor growth inhibitory effect, with similar IC_{50} values in $p53^{+/+}$ (0.98 ± 0.12 μM) and $p53^{-/-}$ (0.68 ± 0.08 μM) HCT116 cells. In HCT116 $p53^{-/-}$ cells, further analysis revealed that 2 μM LEM2 induced G_2/M-phase cell cycle arrest (Fig. 1C) and apoptosis (demonstrated by the increase in Annexin V-positive cells (Fig. 1D) and PARP cleavage (Fig. 1E)). Consistently, in a 3D-model of HCT116 $p53^{-/-}$ cells, 0.5–2 μM LEM2 also markedly inhibited spheroid growth (Fig. 1F) and prevented their formation, when added upon seeding (Fig. 1G).

We next interrogated whether the antiproliferative effect of LEM2 was associated with induction of DNA damage. However, compared to solvent, and unlike the positive controls, 1 and 2 μM LEM2 did not increase the number of micronuclei in human lymphocytes (Fig. 1H), nor the percentage of comet-positive HCT116 $p53^{-/-}$ cells (Fig. 1I and J).

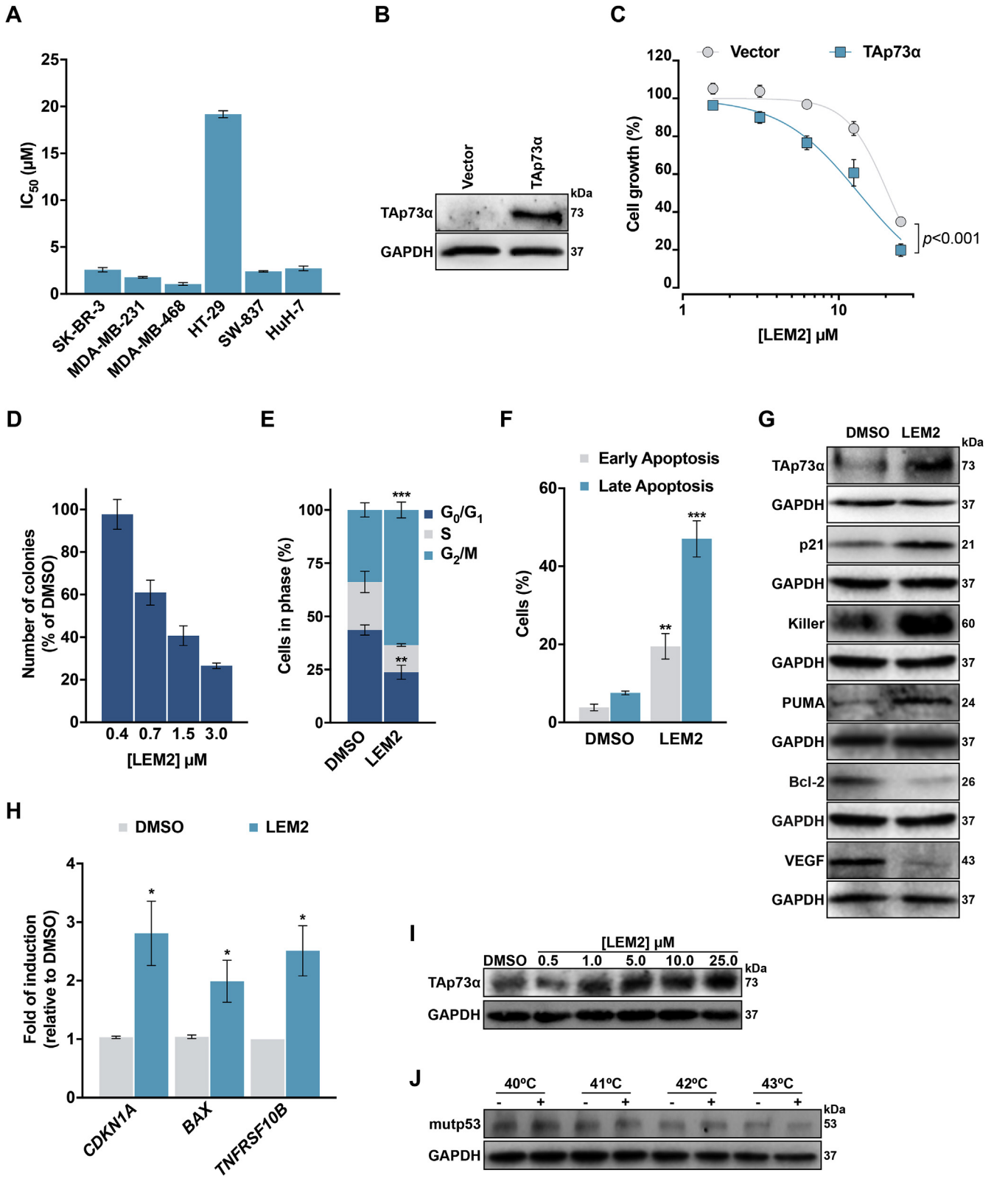

(caption on next page)

3.2. LEM2 has TAp73-dependent growth inhibitory activity in human tumor cells, activating TAp73 through disruption of its interaction with MDM2

A western blot analysis revealed that LEM2-induced growth inhibition in HCT116 $p53^{-/-}$ cells was associated with regulation of several p53-family transcriptional targets. In fact, 1 μM LEM2 increased the protein levels of TAp73α, MDM2, p21, Killer, and Bax, while reducing Bcl-2 and vascular endothelial growth factor (VEGF) protein levels (Fig. 2A). Accordingly, 2 μM LEM2 increased the mRNA levels of *CDKN1A*, *BAX*, *TNFRSF10B*, and *MDM2* (Fig. 2B). Since HCT116 $p53^{-/-}$ cells do not express p53 nor p63 [49] (Fig. S2), we hypothesized that LEM2 growth inhibitory activity in these cells might relate to

Fig. 3. LEM2 has TAp73-dependent growth inhibitory activity in human mutp53-expressing tumor cells, activating TAp73 transcriptional activity and inducing its thermal stabilization. (A) IC_{50} values of LEM2 in human tumor cells expressing different mutp53 forms, determined by SRB assay, after 48 h treatment with 0.39–25.0 μM LEM2. Data are mean ± SEM (n = 4). (B) Protein levels of TAp73α in HT-29 cells transfected with the pCI-neo plasmid encoding TAp73α or with the empty-vector, visualized by western blot. Immunoblots represent one of three independent experiments; GAPDH was used as a loading control. (C) Dose-response curves for the growth inhibitory activity of LEM2 in human HT-29 transfected with the pCI-neo plasmid encoding TAp73α or with the empty vector, determined by SRB assay, after 48 h treatment with 0.39–25.0 μM LEM2. Data are mean ± SEM (n = 4); $p < 0.001$, extra sum-of-squares F test. (D) Effect of LEM2 on the colony formation of MDA-MB-468 cells. Cells were treated with LEM2 or solvent for 24 h, and colonies were allowed to grow for 10 days. Data are mean ± SEM (n = 3). (E) Effect of 1.5 μM LEM2 on cell cycle progression of MDA-MB-468 cells after 24 h treatment. Data are mean ± SEM (n = 3); values significantly different from DMSO: $^{**}p < 0.01$, $^{***}p < 0.001$ (two-way ANOVA with Dunnett's multiple comparison test). (F) Effect of 1.5 μM LEM2 on apoptosis of MDA-MB-468 cells after 48 h treatment. Data are mean ± SEM (n = 4); values significantly different from DMSO: $^{**}p < 0.01$, $^{***}p < 0.001$ (one-way ANOVA with Dunnett's multiple comparison test). (G) Protein levels of TAp73 transcriptional targets in MDA-MB-468 cells, after 16 h (PUMA and TAp73α), 24 h (VEGF), or 48 h (p21, Killer, Bcl-2) treatment with 1.5 μM LEM2 or solvent, visualized by western blot. Immunoblots represent one of three independent experiments; GAPDH was used as a loading control. (H) mRNA levels of TAp73 transcriptional targets measured by RT-qPCR in MDA-MB-468 cells after 24 h (*MDM2*) or 48 h (*BAX* and *TNFRSF10B)* treatment with 2 μM LEM2 or solvent. Fold of induction is relative to solvent. Data are mean ± SEM (n = 3); values significantly different from solvent: $^{*}p < 0.05$, $^{**}p < 0.01$, $^{***}p < 0.001$ (two-way ANOVA with Dunnett's multiple comparison test). (I,J) CETSA in MDA-MB-468 cell lysates treated with LEM2 (+) or solvent (−); soluble protein was analyzed by western blot. In I, lysate samples were treated with 0.5–25 μM LEM2 and heated at 52 °C. In J, lysate samples were treated with 25 μM LEM2 and heated at increasing temperatures.

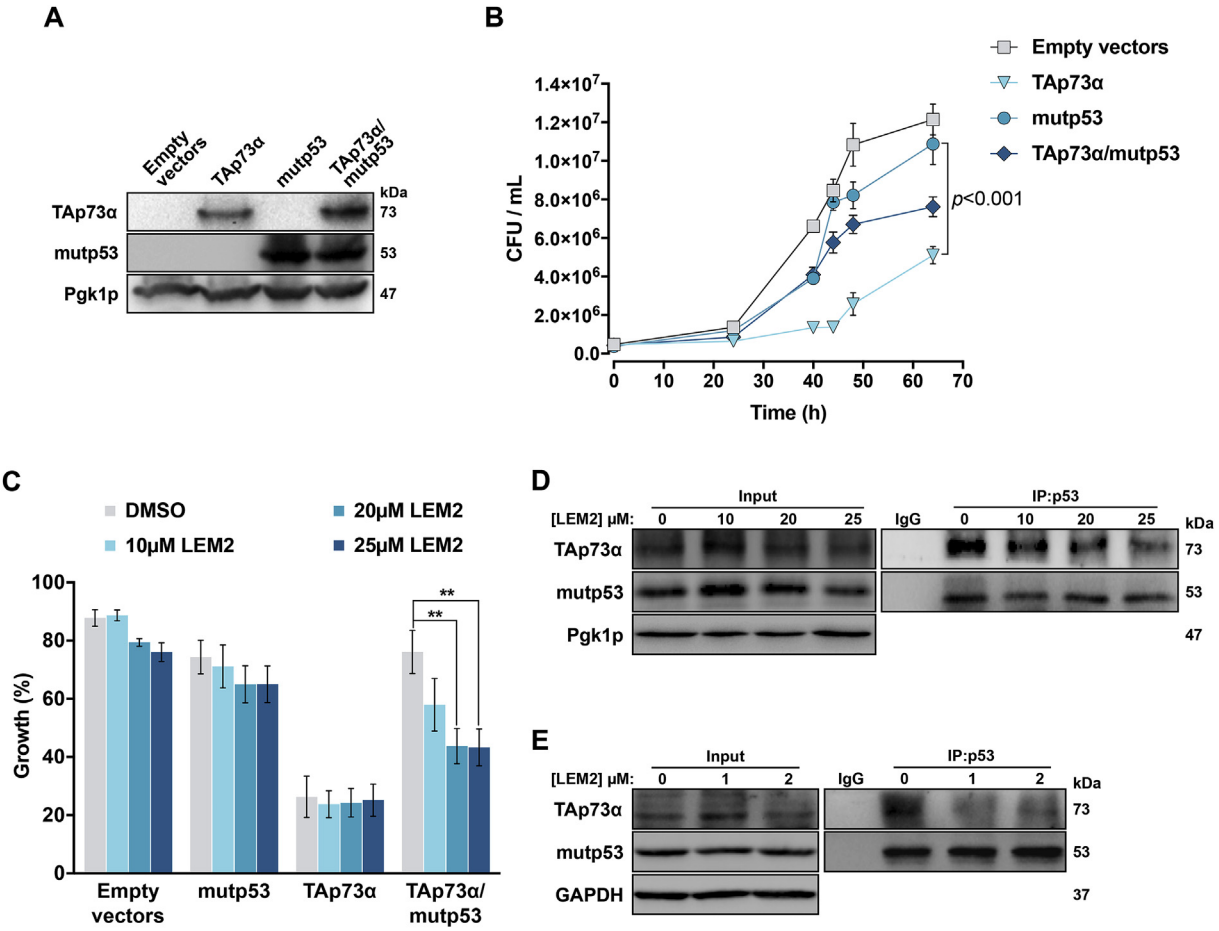

Fig. 4. LEM2 disrupts the TAp73 interaction with mutp53 in yeast and human mutp53-expressing tumor cells. (A) Expression of TAp73α alone and combined with mutp53 in yeast was confirmed by western blot. (B) Yeast cells individually expressing TAp73α or mutp53-R273H, co-expressing TAp73α and mutp53-R273H, and control yeast (empty vectors) were grown for up to 64 h. Growth curves were obtained by CFU counts; data are mean ± SEM (n = 5). (C) Effect of LEM2 on yeast cells individually expressing TAp73α or mutp53-R273H, co-expressing TAp73α and mutp53-R273H, and control yeast. Yeast cells were treated with LEM2 or solvent for 44 h. Results are plotted setting the growth of untreated yeast as 100%. Data are mean ± SEM (n = 4); values significantly different from DMSO: $^{**}p < 0.01$ (one-way ANOVA with Dunnett's multiple comparison test). (D) Co-immunoprecipitation in yeast cells co-expressing TAp73α and mutp53-R273H treated with LEM2 or solvent for 44 h, using anti-immunoglobulin G (IgG) or anti-p53 (IP:p53) antibodies, followed by immunoblotting with anti-TAp73α and anti-p53 antibodies. (E) Co-immunoprecipitation in MDA-MB-468 cells treated with LEM2 or solvent for 24 h, using anti-immunoglobulin G (IgG) or anti-p53 (IP:p53) antibodies, followed by immunoblotting with anti-TAp73α and anti-p53 antibodies. In A, D and E, immunoblots represent one of three independent experiments; Pgk1p (A,D) or GAPDH (E) were used as loading controls.

interference with p73. To test such hypothesis, p73-silenced HCT116 $p53^{-/-}$ cells were obtained using siRNA (Fig. S3A). By colony formation assay, we observed that p73-silenced cells were less susceptible to the inhibitory effect of LEM2 than cells transfected with control siRNA (Fig. 2C). These results supported a p73-dependent growth inhibitory activity of LEM2 in HCT116 $p53^{-/-}$ cells.

Since MDM2 is a well-known inhibitor of TAp73, we investigated the potential mode of action of LEM2 by testing its impact on the

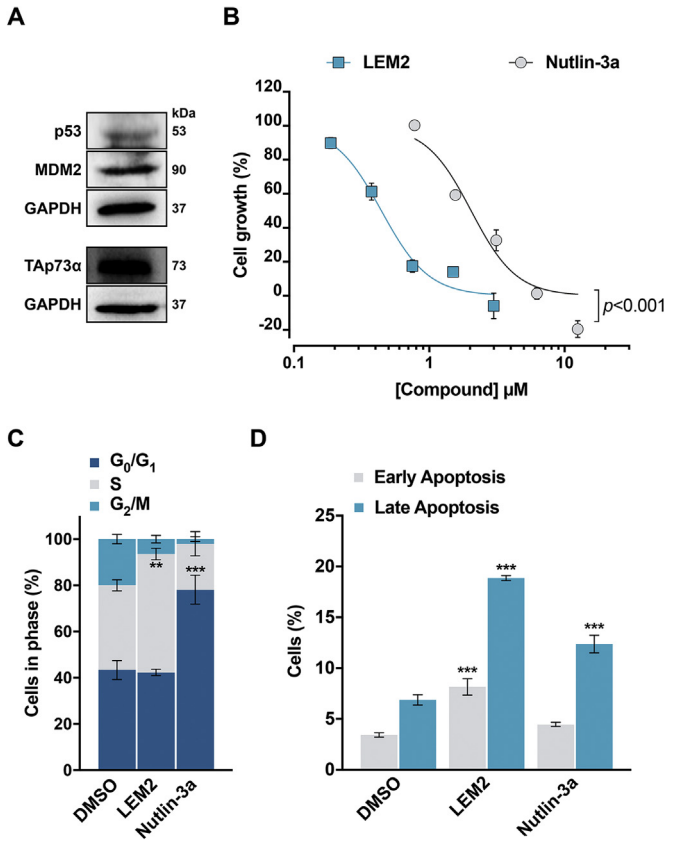

Fig. 5. LEM2 inhibits the growth of NBL cells through induction of cell cycle arrest and apoptosis. (A) Expression of p53, MDM2 and TAp73α, in SH-SY5Y cells, visualized by western blot; immunoblots represent one of three independent experiments; GAPDH was used as a loading control. (B) Dose-response curves for the growth inhibitory activity of 0.18–3.00 μM LEM2 and 0.78–12.5 μM nutlin-3a in SH-SY5Y cells determined by MTT assay, after 48 h treatment. Data are mean ± SEM (n = 4); $p < 0.001$, extra sum-of-squares F test. (C) Effect of 1 μM LEM2 and 4 μM nutlin-3a on cell cycle progression of SH-SY5Y cells after 48 h treatment. Data are mean ± SEM (n = 3); values significantly different from DMSO: $^{**}p < 0.01$, $^{***}p < 0.001$ (two-way ANOVA with Dunnett's multiple comparison test). (D) Effect of 1 μM LEM2 and 4 μM nutlin-3a on apoptosis of SH-SY5Y cells after 48 h treatment. Data are mean ± SEM (n = 4); values significantly different from DMSO: $^{***}p < 0.001$ (one-way ANOVA with Dunnett's multiple comparison test).

TAp73α-MDM2 interaction. For this, we first used a previously developed yeast assay [42]. In this assay, TAp73α-MDM2 interaction inhibitor would restore the TAp73α-induced yeast growth inhibition previously abolished by MDM2. Consistently, LEM2 caused dose-dependent growth inhibition in yeast cells co-expressing TAp73α and MDM2, while not interfering with the growth of control yeast (empty-vectors) and yeast expressing TAp73α or MDM2 alone (Fig. 2D). To confirm these results, co-immunoprecipitation was performed. As expected, 4 and 5 μM LEM2 markedly reduced the amount of MDM2 precipitated with TAp73α (Fig. 2E), while not affecting the amount of MDM2 precipitated with p53 in HCT116 $p53^{+/+}$ cells (Fig. 2F). These results corroborated the ability of LEM2 to disrupt the TAp73α-MDM2 interaction, having a p53-independent growth inhibitory effect in tumor cells. Additionally, it was verified by CETSA that 5–25 μM LEM2 induced thermal stabilization of TAp73α at 56 °C in HCT116 $p53^{-/-}$ cells (Fig. 2G). Conversely, LEM2 did not increase the melting temperature of MDM2, even at the concentration that caused maximum TAp73α thermal stabilization (25 μM) (Fig. 2H). These data supported a potential interference of LEM2 with TAp73α and not with MDM2.

3.3. LEM2 has TAp73-dependent growth inhibitory activity in mutp53-expressing human tumor cells, activating TAp73 through disruption of its interaction with mutp53

The effect of LEM2 on the growth of human tumor cells expressing distinct mutp53 forms was also investigated by SRB assay (Fig. 3A). The IC_{50} values (around 1–3 μM) revealed a potent antiproliferative effect of LEM2 against SK-BR-3 (mutp53-R175H), MDA-MB-231 (mutp53-R280K), MDA-MB-468 (mutp53-R273H), SW-837 (mutp53-R248W), and HuH-7 (mutp53-Y220C) cells. The only exception were HT-29 cells (mutp53-R273H), in which the IC_{50} of LEM2 (20 μM) was much higher than those in the remaining mutp53-expressing tumor cells, particularly in MDA-MB-468 cells (1.5 μM), which express the same mutp53 (Fig. 3A). Interestingly, in HT-29 cells, TAp73α protein levels are much lower than in MDA-MB-468 cells (Fig. S3B). This raised the hypothesis that, in mutp53-expressing tumor cells, LEM2 antiproliferative activity might also be mediated by TAp73 activation. In fact, the ectopic expression of TAp73α in HT-29 cells (Fig. 3B) significantly enhanced LEM2 antiproliferative activity (Fig. 3C). Consistently, in MDA-MB-468 cells, the pronounced LEM2 growth inhibitory activity observed by SRB (Fig. 3A) and colony formation (Fig. 3D) assay, was associated with pronounced G_2/M-phase cell cycle arrest (Fig. 3E) and apoptosis (Fig. 3F), and regulation of several TAp73 transcriptional targets. In fact, in these cells, 1.5 μM LEM2 increased TAp73α, p21, Killer, and PUMA protein levels, while decreasing Bcl-2 and VEGF (Fig. 3G). Likewise, LEM2 increased mRNA levels of *CDKN1A*, *BAX,* and *TNFRSF10B* in MDA-MB-468 cells (Fig. 3H). In MDA-MB-468 cells, the involvement of TAp73α in LEM2 growth inhibitory activity was further supported by CETSA. In this assay, 1–25 μM LEM2 induced TAp73α thermal stabilization at 52 °C (Fig. 3I), while no increase in the mutp53 melting temperature was observed even at the concentration that caused maximum TAp73α thermal stabilization (25 μM) (Fig. 3J). Collectively, these results supported the involvement of TAp73 in LEM2 growth inhibitory activity in mutp53-expressing tumor cells.

Since mutp53 interacts with and inhibits TAp73, we interrogated whether LEM2 would also disrupt the TAp73-mutp53 interaction. To answer this question, we developed a new yeast assay, consisting of yeast cells expressing human TAp73α and/or mutp53-R273H, and control yeast (empty-vectors) (Fig. 4A). In this assay, TAp73α expression induced marked yeast growth inhibition, which was reverted by co-expression with mutp53 (Fig. 4B). As such, a reestablishment of TAp73α-induced yeast growth inhibition would reflect the disruption of its interaction with mutp53. This was obtained with 20 and 25 μM LEM2 in yeast cells co-expressing TAp73α and mutp53-R273H, while no effect was observed in control yeast or yeast expressing TAp73α or mutp53 alone (Fig. 4C). To confirm that the reestablishment of TAp73α-induced yeast growth inhibition by LEM2 was due to disruption of the TAp73α-mutp53 interaction, co-immunoprecipitation was performed. In this assay, 10–25 μM LEM2 visibly decreased the amount of TAp73α precipitated with mutp53 in yeast (Fig. 4D).

Consistently, in MDA-MB-468 cells, 1 and 2 μM LEM2 also visibly decreased the amount of TAp73α precipitated with mutp53, further supporting the ability of LEM2 to disrupt the TAp73α-mutp53 interaction in human tumor cells (Fig. 4E).

3.4. LEM2 has TAp73-dependent growth inhibitory activity in NBL cells, sensitizing these cells to the effect of conventional chemotherapeutics

Considering the crucial role of TAp73 in NBL tumorigenesis [31], the antitumor activity of LEM2 against NBL cells was investigated. To this end, the growth inhibitory effect of LEM2 against SH-SY5Y cells, expressing TAp73α, wtp53 (Fig. 5A) [50] and MDM2 (Fig. 5A), was assessed. In these cells, LEM2 displayed potent growth inhibitory effect (IC_{50} = 0.50 ± 0.03 μM; Fig. 5B), associated with S-phase cell cycle arrest (Fig. 5C) and apoptosis (Fig. 5D). Notably, this effect was significantly higher than that of nutlin-3a (Fig. 5B), a known disruptor of

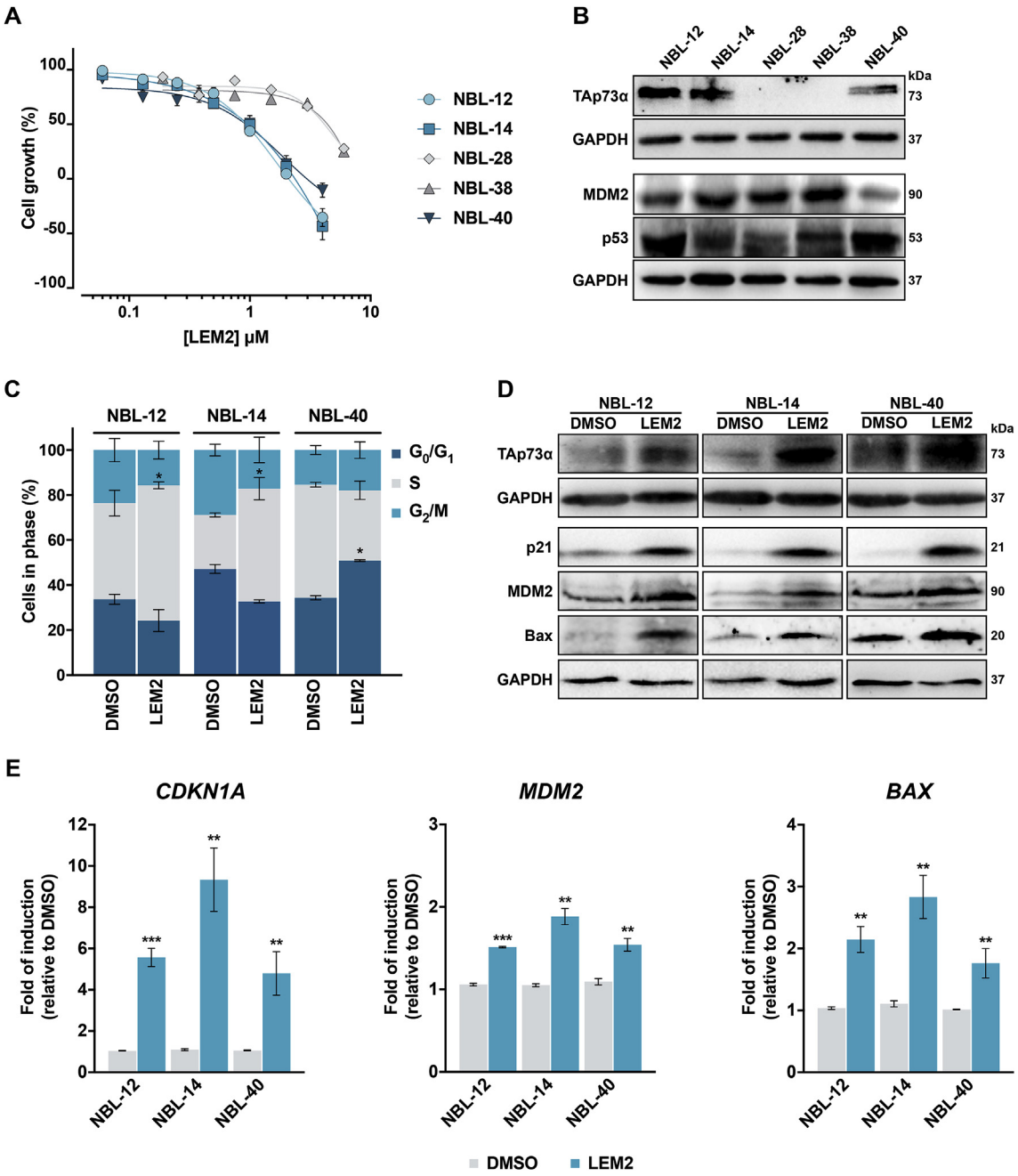

Fig. 6. LEM2 has TAp73-dependent growth inhibitory activity in patient-derived NBL cells through regulation of TAp73 transcriptional targets. (A) Dose-response curves for the growth inhibitory activity of 0.125–6.00 µM LEM2 in five patient-derived NBL cell lines, determined by MTT assay, after 48 h treatment. Data are mean ± SEM (n = 5). (B) Expression of TAp73α, p53 and MDM2 in patient-derived NBL cells visualized by western blot. (C) Effect of 1.4 µM LEM2 on cell cycle progression of NBL-12, NBL-14, and NBL-40 cells after 48 h treatment. Data are mean ± SEM (n = 3); values significantly different from DMSO: $*p < 0.05$ (two-way ANOVA with Dunnett's multiple comparison test). (D) Protein levels of TAp73 transcriptional targets in NBL-12, NBL-14, and NBL-40 cells, after 24 h treatment with 1.4 µM LEM2, visualized by western blot. (E) mRNA levels of TAp73 transcriptional targets measured by RT-qPCR in NBL-12, NBL-14, and NBL-40 cells after 24 h treatment with 1.4 µM LEM2. Fold of induction is relative to solvent. Data are mean ± SEM (n = 3); values significantly different from solvent: $*p < 0.05$; $**p < 0.01$, $***p < 0.001$ (two-way ANOVA with Dunnett's multiple comparison test). In B and D, immunoblots represent one of three independent experiments; GAPDH was used as loading control.

the TAp73-MDM2 interaction [19] with antitumor activity against NBL cells [51].

The antitumor potential of LEM2 was also tested in five human patient-derived NBL cells expressing wtp53 (p53 status was determined by FASAY assay; Table S3). In MTT assay, LEM2 reduced cell viability of all NBL cells, although this effect was less pronounced for NBL-28 and NBL-38 (Fig. 6A). Interestingly, although all NBL cells expressed p53 and MDM2 (Fig. 6B), no TAp73α protein (Fig. 6B) or mRNA (Fig. S4) expression was detected in NBL-28 and NBL-38 cells.

In TAp73α-expressing NBL cells, the IC_{50} (1.4 µM) of LEM2 induced G_0/G_1- (NBL-40) or S-phase (NBL-12 and NBL-14) cell cycle arrest (Fig. 6C). Additionally, it increased TAp73α protein levels, as well as protein (Fig. 6D) and mRNA (Fig. 6E) levels of its transcriptional targets p21 (*CDKN1A*), MDM2, and Bax.

The ability of LEM2 to sensitize SH-SY5Y and patient-derived NBL-14 cells to the effect of DOXO and cisplatin was also assessed by MTT

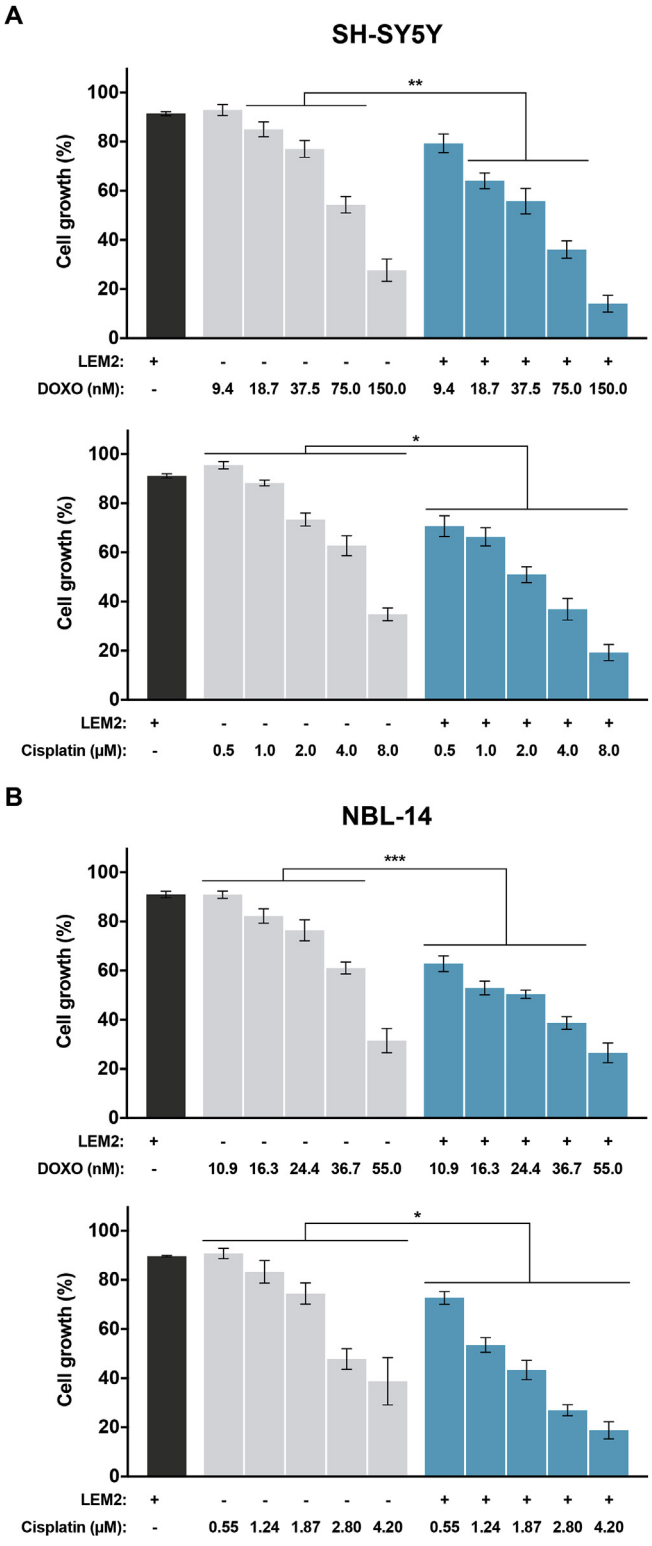

Fig. 7. LEM2 sensitizes NBL cells to the effect of DOXO and cisplatin. (A) SH-SY5Y and (B) patient-derived NBL-14 cells were treated with increasing concentrations of DOXO/cisplatin, alone and in combination with 0.21 μM (in SH-SY5Y cells) or 0.48 μM (in patient-derived NBL-14 cells) LEM2; cell viability was assessed by MTT assay after 48 h treatment; data are mean ± SEM (n = 5); values significantly different from chemotherapeutic alone: *$p < 0.05$, **$p < 0.01$, ***$p < 0.001$ (two-way ANOVA with Sidak's multiple comparison test).

Table 1
Effect of LEM2 in combination with conventional chemotherapeutics, in SH-SY5Y and patient-derived NBL-14 cells.

Drug combination with LEM2	Mutually nonexclusive CI		Dose reduction index (DRI)
	CI	Profile	
SH-SY5Y cells			
DOXO (nM)			
9.37	1.007	Additive	2.911
18.7	0.859	Synergy	2.688
37.5	0.987	Synergy	1.776
75	0.896	Synergy	1.696
150	0.619	Synergy	2.310
Cisplatin (μM)			
0.5	0.803	Synergy	5.120
1	0.899	Synergy	3.003
2	0.860	Synergy	2.470
4	0.889	Synergy	1.948
8	0.787	Synergy	1.949
Patient-derived NBL-14 cells			
DOXO (nM)			
10.9	0.655	Synergy	3.101
16.3	0.665	Synergy	2.459
24.4	0.827	Synergy	1.713
36.7	0.901	Synergy	1.389
55	0.984	Synergy	1.168
Cisplatin (μM)			
0.55	0.938	Synergy	3.557
1.24	0.889	Synergy	2.561
1.87	0.892	Synergy	2.177
2.8	0.780	Synergy	2.256
4.2	0.787	Synergy	1.998

The synergistic effect of LEM2 at 0.21 μM (in SH-SY5Y cells) and 0.48 μM (in NBL-14 cells), in combination with DOXO or cisplatin, was evaluated using CompuSyn software to calculate combination index (CI) and conventional chemotherapeutic dose reduction index (DRI) values for each combined treatment. CI < 1, synergy; 1 < CI < 1.1, additive effect; CI > 1.1, antagonism. Data were calculated using a mean value effect (n = 5).

assay. Cells were treated with increasing concentrations of each conventional chemotherapeutic, alone or in combination with LEM2 (at a concentration with no significant effect on cell growth; 0.21 μM in SH-SY5Y cells, 0.48 μM in NBL-14 cells). The combination of DOXO/cisplatin with LEM2 significantly increased cytotoxicity compared to chemotherapeutic drugs alone, in SH-SY5Y (Fig. 7A) and NBL-14 (Fig. 7B) cells. In fact, except for 9.37 nM DOXO in SH-SY5Y cells, a synergistic effect (CI < 1) was obtained for all tested combination therapies, in both SH-SY5Y and NBL-14 cells (Table 1). Furthermore, the DRI > 1 showed a potential reduction of the effective dose of conventional chemotherapeutics by LEM2 (Table 1).

4. Discussion

TAp73 is a key tumor suppressor protein, particularly in p53-disrupted tumor cells. Besides its ability to transactivate p53 target genes, regulating cellular processes as cell cycle and apoptosis, additional tumor suppressor properties have been attributed to TAp73, which are not shared by p53 [5]. This has strengthened the concept of functional replacement of impaired p53 by TAp73 in anticancer therapy [17].

Xanthones are a relevant class of *O*-heterocycles in Medicinal Chemistry, with several representatives in clinical research [52]. Herein, we report the xanthonic derivative LEM2, as a new TAp73 activator with potent antitumor activity. In p53-null and mutp53-expressing tumor cells, LEM2 displayed pronounced TAp73-dependent antiproliferative effect through cell cycle arrest and apoptosis. Moreover, it inhibited the growth of tumor cell spheroids, with no genotoxicity. Interestingly, in these cells, LEM2 downregulated the angiogenesis-inducing factor VEGF, suggesting a potential antiangiogenic activity.

In an attempt to further understand its mechanism of TAp73 activation, LEM2 was shown to disrupt the TAp73 interaction with MDM2 and mutp53, both in yeast and in human tumor cells. It is of note that first evidences are provided in this work supporting the suitability of the yeast model to screen for TAp73 activators, particularly TAp73-mutp53 interaction inhibitors. The peculiar ability of LEM2 to inhibit both the TAp73-MDM2 and TAp73-mutp53 interactions may be explained by its possible interference with TAp73, as evidenced by LEM2-induced TAp73 thermal stabilization. This dual LEM2 activity allows to predict promising therapeutic applications in a wide variety of cancer types. Additionally, since normal cells typically express low TAp73 levels, its activation by release of inhibitory interactions has been proposed as a selective anticancer therapeutic strategy, with minimal toxicity on normal cells [6].

Cells have the ability to metabolize aldehydes, a process largely dependent on the aldehyde and on the cellular content of aldehyde-metabolizing enzymes, being reduction and oxidation the major metabolic routes for aromatic aldehydes [53]. Therefore, it could be hypothesized that the alcohol and/or carboxylic acid derivatives of LEM2 might be the active species responsible for TAp73 activation, instead of LEM2 itself. To test this hypothesis, the biological activity of the alcohol 1-(hydroxymethyl)-3,4-dimethoxy-9*H*-xanthen-9-one (LEMred) and the carboxylic acid 3,4-dimethoxy-9-oxo-9*H*-xanthene-1-carboxylic acid (LEMox) putative metabolites of LEM2 (Supplementary Materials and Methods) was evaluated. In yeast, none of the two compounds was able to inhibit the TAp73-MDM2 interaction (Fig. S5A). Concerning the TAp73-mutp53 interaction, although a significant inhibitory effect was observed with LEMred, its activity was much lower than that obtained with LEM2 (Fig. S5B). Most importantly, both compounds displayed weak antitumor activity, with much higher IC_{50} values (superior to 25 μM, maximal concentration tested) than LEM2 in both HCT116 $p53^{-/-}$ and MDA-MB-468 tumor cells (Fig. S5C). These results support that the biological activity obtained with LEM2 treatment can be attributed to the molecule itself and not to its alcohol and carboxylic acid derivatives.

Accumulating data have supported the crucial role of TAp73 in NBL development and progression. In fact, besides its p53-like tumor suppressive activity, TAp73 also promotes p53 nuclear translocation from the cytoplasm (where it is inactivated), in NBL cells [54]. Additionally, TAp73 downregulates N-myc [50], an oncoprotein commonly associated with high-risk and poor prognosis of NBL [55,56]. Interestingly, TAp73 also plays a preponderant role in neuronal differentiation [57], inducing NBL cell differentiation [58]. Since LEM2 is a TAp73 activator, we investigated its antitumor potential towards NBL cells. As expected, in immortalized NBL cells, LEM2 displayed potent antitumor activity, superior to that of nutlin-3a. Most importantly, the potent TAp73-dependent LEM2 cytotoxic activity was also confirmed in patient-derived NBL cells, allowing to predict about its effective clinical translation.

Current chemotherapeutic regimens against NBL, particularly high-risk NBL, include DOXO and cisplatin in intensive induction therapy, followed by high-dose myeloablative consolidation therapy [59,60]. Interestingly, both DOXO and cisplatin induce proteasomal degradation of ΔNp73 [59,61], which is commonly overexpressed in NBL relating to poor prognosis particularly due to its dominant-negative effect on TAp73 transcriptional activity [26,62]. However, these regimens have been associated with significant toxic side effects, and frequent relapse after remission [60]. The sensitization of NBL cells to these chemotherapeutics is a promising therapeutic approach, reducing NBL resistance and minimizing the toxicity associated with high doses of these agents. Herein, we report pronounced synergistic effects between DOXO/cisplatin and LEM2, which may result from enhancing TAp73 activation through alternative pathways. Consistently, nutlin-3a-induced TAp73 activation has also been reported to enhance the effect of conventional chemotherapeutics in NBL [32,61].

In conclusion, despite the relevance of TAp73 in anticancer therapy, effective TAp73-activating agents are still mostly unavailable. In this work, we report the TAp73-activating agent LEM2 capable of inhibiting the TAp73 interaction with both MDM2 and mutp53. The potent antitumor activity of LEM2 towards primary patient-derived NBL cells, both alone and in combination with conventional chemotherapeutics, may predict promising clinical applications in NBL therapy.

Conflicts of interest statement

All authors confirm that they do not have any conflict of interest to disclose.

Author contribution

SG, LR, JS, performed experiments, analyzed the data, and wrote the manuscript; JBL, ML, HR, MNM, contributed to the experimental work; PC, RV, coordinated the experimental work with human patient-derived NBL cell lines; MP, ES, conceived the design and synthesis of LEM2; AL, JM, synthesized LEMred and LEMox; LS, conceived and designed the study, provided financial support for the study, analyzed the data, wrote the manuscript. All authors read and approved the final version of the manuscript.

Funding

This work was supported by European Union (FEDER funds POCI/01/0145/FEDER/007728 through Programa Operacional Factores de Competitividade – COMPETE) and National Funds (FCT/MEC, Fundação para a Ciência e Tecnologia and Ministério da Educação e Ciência) under the Partnership Agreement PT2020 UID/MULTI/04378/2013 and the projects (3599-PPCDT) PTDC/DTP-FTO/1981/2014 – POCI-01-0145-FEDER-016581, POCI-01-0145-FEDER-028736, and (3599-PPCDT) PTDC/MAR-BIO/4694/2014-POCI-01-0145-FEDER-016790; by the National Program of Sustainability II (MEYS CR) - Project Translational Medicine LQ1605 and by Masaryk University (MUNI/A/0824/2017). We also thank FCT for the financial support through fellowships SFRH/BD/96189/2013 (S. Gomes), SFRH/BD/117949/2016 (L. Raimundo), SFRH/BD/119144/2016 (H. Ramos), SFRH/BD/128673/2017 (J. B. Loureiro), and the Programa Operacional Potential Humano (POCH), specifically the BiotechHealth Programme (Doctoral Programme on Cellular and Molecular Biotechnology Applied to Health Sciences; PD/00016/2012).

Acknowledgements

We thank Dr Alberto Inga (Centre for Integrative Biology, University of Trento, Italy) for providing the pCI-neo, pCI-neo-TAp73α, pRS314, and pRS314-TAp73α plasmids; Dr Gilberto Fronza (IST Istituto Nazionale per la Ricerca sul Cancro, Italy) for providing the pLS76 and pLS76-mutp53-R273H plasmids; Dr Marco G. Alves and Bruno Moreira for aiding with the RT-qPCR assays; Dr Jana Smardova (Department of Pathology, University Hospital and Department of Experimental Biology, Faculty of Science, Masaryk University, Brno, Czech Republic) for FASAY analysis of patient-derived NBL cells.

Appendix A. Supplementary data

Supplementary data to this article can be found online at https://doi.org/10.1016/j.canlet.2019.01.014.

References

[1] M.S. Sheikh, A.J. Fornace, Role of p53 family members in apoptosis, J. Cell. Physiol. 182 (2000) 171–181 https://doi.org/10.1002/(SICI)1097-4652(200002)182:2%3c171::AID-JCP5%3e3.0.CO;2-3.

[2] E. Candi, M. Agostini, G. Melino, F. Bernassola, How the TP53 family proteins TP63 and TP73 contribute to tumorigenesis: regulators and effectors, Hum. Mutat. 35 (2014) 702–714 https://doi.org/10.1002/humu.22523.

[3] C.A. Jost, M.C. Marin, W.G. Kaelin Jr., p73 is a simian [correction of human] p53-related protein that can induce apoptosis, Nature 389 (1997) 191–194 https://doi.org/10.1038/38298.

[4] M. Kaghad, H. Bonnet, A. Yang, L. Creancier, J.-C. Biscan, A. Valent, A. Minty, P. Chalon, J.M. Lelias, X. Dumont, P. Ferrara, F. McKeon, D. Caput, Monoallelically expressed gene related to p53 at 1p36, a region frequently deleted in neuroblastoma and other human cancers, Cell 90 (1997) 809–819 https://doi.org/10.1016/S0092-8674(00)80540-1.

[5] C.J. Di Como, C. Gaiddon, C. Prives, p73 function is inhibited by tumor-derived p53 mutants in mammalian cells, Mol. Cell Biol. 19 (1999) 1438–1449 https://doi.org/0.1128/MCB.19.2.1438.

[6] A.M. Maas, A.C. Bretz, E. Mack, T. Stiewe, Targeting p73 in cancer, Cancer Lett. 332 (2013) 229–236 https://doi.org/10.1016/j.canlet.2011.07.030.

[7] M.S. Irwin, K. Kondo, M.C. Marin, L.S. Cheng, W.C. Hahn, W.G. Kaelin, Chemosensitivity linked to p73 function, Cancer Cell 3 (2003) 403–410 https://doi.org/10.1016/S1535-6108(03)00078-3.

[8] K. Inoue, E.A. Fry, Alterations of p63 and p73 in human cancers, Subcell. Biochem. 85 (2014) 17–40 https://doi.org/10.1007/978-94-017-9211-0_2.

[9] W.A. Freed-Pastor, C. Prives, Mutant p53: one name, many proteins, Genes Dev. 26 (2012) 1268–1286 https://doi.org/10.1101/gad.190678.112.

[10] M.C. Marin, C.A. Jost, L.A. Brooks, M.S. Irwin, J. O'Nions, J.A. Tidy, N. James, J.M. McGregor, C.A. Harwood, I.G. Yulug, K.H. Vousden, M.J. Allday, B. Gusterson, S. Ikawa, P.W. Hinds, T. Crook, W.G. Kaelin, A common polymorphism acts as an intragenic modifier of mutant p53 behaviour, Nat. Genet. 25 (2000) 47–54 https://doi.org/10.1038/75586.

[11] P. Monti, P. Campomenosi, Y. Ciribilli, R. Iannone, A. Aprile, A. Inga, M. Tada, P. Menichini, A. Abbondandolo, G. Fronza, Characterization of the p53 mutants ability to inhibit p73β transactivation using a yeast-based functional assay, Oncogene 22 (2003) 5252–5260 https://doi.org/10.1038/sj.onc.1206511.

[12] P.A.J. Muller, P.T. Caswell, B. Doyle, M.P. Iwanicki, E.H. Tan, S. Karim, N. Lukashchuk, D.A. Gillespie, R.L. Ludwig, P. Gosselin, A. Cromer, J.S. Brugge, O.J. Sansom, J.C. Norman, K.H. Vousden, Mutant p53 drives invasion by promoting integrin recycling, Cell 139 (2009) 1327–1341 https://doi.org/10.1016/j.cell.2009.11.026.

[13] E. Bálint, S. Bates, K.H. Vousden, Mdm2 binds p73 alpha without targeting degradation, Oncogene 18 (1999) 3923–3929 https://doi.org/10.1038/sj.onc.1202781.

[14] N. Kubo, R. Okoshi, K. Nakashima, O. Shimozato, A. Nakagawara, T. Ozaki, MDM2 promotes the proteasomal degradation of p73 through the interaction with Itch in HeLa cells, Biochem. Biophys. Res. Commun. 403 (2010) 405–411 https://doi.org/10.1016/j.bbrc.2010.11.043.

[15] S. Strano, E. Munarriz, M. Rossi, B. Cristofanelli, Y. Shaul, L. Castagnoli, A.J. Levine, A. Sacchi, G. Cesareni, M. Oren, G. Blandino, Physical and Functional Interaction between p53 Mutants and Different Isoforms of p73, J. Biol. Chem. 275 (2000) 29503–29512 https://doi.org/10.1074/jbc.M003360200.

[16] X. Zeng, L. Chen, C.A. Jost, R. Maya, D. Keller, X. Wang, W.G. Kaelin, M. Oren, J. Chen, H. Lu, MDM2 suppresses p73 function without promoting p73 degradation, Mol. Cell Biol. 19 (1999) 3257–3266 https://doi.org/10.1128/MCB.19.5.3257.

[17] H. Wu, R.P. Leng, MDM2 mediates p73 ubiquitination: a new molecular mechanism for suppression of p73 function, Oncotarget 6 (2015) 21479–21492 https://doi.org/10.18632/oncotarget.4086.

[18] L.T. Vassilev, B.T. Vu, B. Graves, D. Carvajal, F. Podlaski, Z. Filipovic, N. Kong, U. Kammlott, C. Lukacs, C. Klein, N. Fotouhi, E.A. Liu, In vivo activation of the p53 pathway by small-molecule antagonists of MDM2, Science 303 (2004) 844–848 https://doi.org/10.1126/science.1092472.

[19] L.M. Lau, J.K. Nugent, X. Zhao, M.S. Irwin, HDM2 antagonist Nutlin-3 disrupts p73-HDM2 binding and enhances p73 function, Oncogene 27 (2008) 997–1003 https://doi.org/10.1038/sj.onc.1210707.

[20] S. Di Agostino, G. Cortese, O. Monti, S. Dell'Orso, A. Sacchi, M. Eisenstein, G. Citro, S. Strano, G. Blandino, The disruption of the protein complex mutantp53/p73 increases selectively the response of tumor cells to anticancer drugs, Cell Cycle 7 (2008) 3440–3447 https://doi.org/10.4161/cc.7.21.6995.

[21] J.E. Kravchenko, G.V. Ilyinskaya, P.G. Komarov, L.S. Agapova, D.V. Kochetkov, E. Strom, E.I. Frolova, I. Kovriga, A.V. Gudkov, E. Feinstein, P.M. Chumakov, Small-molecule RETRA suppresses mutant p53-bearing cancer cells through a p73-dependent salvage pathway, Proc. Natl. Acad. Sci. U. S. A. 105 (2008) 6302–6307 https://doi.org/10.1073/pnas.0802091105.

[22] B. Hong, V.V. Prabhu, S. Zhang, A.P.J. van den Heuvel, D.T. Dicker, L. Kopelovich, W.S. El-Deiry, Prodigiosin rescues deficient p53 signaling and antitumor effects via upregulating p73 and disrupting its interaction with mutant p53, Cancer Res. 74 (2014) 1153–1165 https://doi.org/10.1158/0008-5472.CAN-13-0955.

[23] B. Xie, A. Nagalingam, P. Kuppusamy, N. Muniraj, P. Langford, B. Győrffy, N.K. Saxena, D. Sharma, Benzyl Isothiocyanate potentiates p53 signaling and antitumor effects against breast cancer through activation of p53-LKB1 and p73-LKB1 axes, Sci. Rep. 7 (2016) 1–14 https://doi.org/10.1038/srep40070.

[24] A.M. Noone, N. Howlader, M. Krapcho, D. Miller, A. Brest, M. Yu, J. Ruhl, Z. Tatalovich, A. Mariotto, D.R. Lewis, H.S. Chen, E.J. Feuer, K.A. Cronin, SEER Cancer Statistics Review, 1975-2015, based on November 2017 SEER Data Submission, Posted to the SEER Web Site, National Cancer Institute, Bethesda, MD, 2018https://seer.cancer.gov/csr/1975_2015/ April 2018.

[25] A. Nakagawara, Y. Li, H. Izumi, K. Muramori, H. Inada, M. Nishi, Neuroblastoma, Jpn. J. Clin. Oncol. 48 (2018) 214–241 https://doi.org/10.1093/jjco/hyx176.

[26] A.Y. Nikolaev, M. Li, N. Puskas, J. Qin, W. Gu, Parc: a cytoplasmic anchor for p53, Cell 112 (2003) 29–40 https://doi.org/10.1016/S0092-8674(02)01255-2.

[27] I. Casciano, K. Mazzocco, L. Boni, G. Pagnan, B. Banelli, G. Allemanni, M. Ponzoni, G.P. Tonini, M. Romani, Expression of DeltaNp73 is a molecular marker for adverse outcome in neuroblastoma patients, Cell Death Differ. 9 (2002) 246–251 https://doi.org/10.1038/sj.cdd.4400993.

[28] A. Slack, Z. Chen, R. Tonelli, M. Pule, L. Hunt, A. Pession, J.M. Shohet, The p53 regulatory gene MDM2 is a direct transcriptional target of MYCN in neuroblastoma, Proc. Natl. Acad. Sci. U. S. A. 102 (2005) 731–736 https://doi.org/10.1073/pnas.0405495102.

[29] K. Vogan, M. Bernstein, J.-M. Leclerc, L. Brisson, J. Brossard, G.M. Brodeur, J. Pelletier, P. Gros, Absence of p53 gene mutations in primary neuroblastomas, Cancer Res. 53 (1993) 5269–5273.

[30] J. Carr, E. Bell, A.D.J. Pearson, U.R. Kees, H. Beris, J. Lunec, D.A. Tweddle, Increased frequency of aberrations in the p53/MDM2/p14(ARF) pathway in neuroblastoma cell lines established at relapse, Cancer Res. 66 (2006) 2138–2145 https://doi.org/10.1158/0008-5472.CAN-05-2623.

[31] J. Wolter, P. Angelini, M. Irwin, p53 family: therapeutic targets in neuroblastoma, Future Oncol. 6 (2010) 429–444 https://doi.org/10.2217/fon.09.176.

[32] S.K. Peirce, H.W. Findley, The MDM2 antagonist nutlin-3 sensitizes p53-null neuroblastoma cells to doxorubicin via E2F1 and TAp73, Int. J. Oncol. 34 (2009) 1395–1402 https://doi.org/10.3892/ijo_00000267.

[33] R. Veselska, M. Hermanova, T. Loja, P. Chlapek, I. Zambo, K. Vesely, K. Zitterbart, J. Sterba, Nestin expression in osteosarcomas and derivation of nestin/CD133 positive osteosarcoma cell lines, BMC Canc. 8 (2008) 300 https://doi.org/10.1186/1471-2407-8-300.

[34] R. Veselska, P. Kuglik, P. Cejpek, H. Svachova, J. Neradil, T. Loja, J. Relichova, Nestin expression in the cell lines derived from glioblastoma multiforme, BMC Canc. 6 (2006) 32 https://doi.org/10.1186/1471-2407-6-32.

[35] J. Soares, N.A. Pereira, A. Monteiro, M. Leao, C. Bessa, D.J.V.A. dos Santos, L. Raimundo, G. Queiroz, A. Bisio, A. Inga, C. Pereira, M.M.M.M. Santos, L. Saraiva, Oxazoloisoindolinones with in vitro antitumor activity selectively activate a p53-pathway through potential inhibition of the p53-MDM2 interaction, Eur. J. Pharm. Sci. 66 (2015) 138–147 https://doi.org/10.1016/j.ejps.2014.10.006.

[36] M. Sramek, J. Neradil, P. Macigova, P. Mudry, K. Polaskova, O. Slaby, H. Noskova, J. Sterba, R. Veselska, Effects of Sunitinib and Other Kinase Inhibitors on Cells Harboring a PDGFRB Mutation Associated with Infantile Myofibromatosis, Int. J. Mol. Sci. 19 (2018) 2599 https://doi.org/10.3390/ijms19092599.

[37] C. Bessa, J. Soares, L. Raimundo, J.B. Loureiro, C. Gomes, F. Reis, M.L. Soares, D. Santos, C. Dureja, S.R. Chaudhuri, C. Lopez-Haber, M.G. Kazanietz, J. Goncalves, M.F. Simoes, P. Rijo, L. Saraiva, Discovery of a small-molecule protein kinase Cdelta-selective activator with promising application in colon cancer therapy, Cell Death Dis. 9 (2018) 23 https://doi.org/10.1038/s41419-017-0154-9.

[38] J. Soares, L. Raimundo, N.A. Pereira, D.J.V.A. dos Santos, M. Perez, G. Queiroz, M. Leao, M.M.M. Santos, L. Saraiva, A tryptophanol-derived oxazolopiperidone lactam is cytotoxic against tumors via inhibition of p53 interaction with murine double minute proteins, Pharmacol. Res. 95–96 (2015) 42–52 https://doi.org/10.1016/j.phrs.2015.03.006.

[39] L. Raimundo, M. Espadinha, J. Soares, J.B. Loureiro, M.G. Alves, M.M.M. Santos, L. Saraiva, Improving anticancer activity towards colon cancer cells with a new p53-activating agent, Br. J. Pharmacol. 175 (2018) 3947–3962 https://doi.org/10.1111/bph.14468.

[40] J. Soares, L. Raimundo, N.A. Pereira, A. Monteiro, S. Gomes, C. Bessa, C. Pereira, G. Queiroz, A. Bisio, J. Fernandes, C. Gomes, F. Reis, J. Goncalves, A. Inga, M.M.M. Santos, L. Saraiva, Reactivation of wild-type and mutant p53 by tryptophanolderived oxazoloisoindolinone SLMP53-1, a novel anticancer small-molecule, Oncotarget 7 (2016) 4326–4343 https://doi.org/10.18632/oncotarget.6775.

[41] M. Leao, C. Pereira, A.M. Baiva, N. Machado, A. Palmeira, M.X. Fernandes, E. Sousa, M. Pinto, A. Inga, L. Saraiva, Discovery of a new small-molecule inhibitor of p53-MDM2 interaction using a yeast-based approach, Biochem. Pharmacol. 85 (2013) 1234–1245 https://doi.org/10.1016/j.bcp.2013.01.032.

[42] M. Leao, S. Gomes, C. Bessa, J. Soares, L. Raimundo, P. Monti, G. Fronza, C. Pereira, L. Saraiva, Studying p53 family proteins in yeast: induction of autophagic cell death and modulation by interactors and small molecules, Exp. Cell Res. 330 (2015) 164–177 https://doi.org/10.1016/j.yexcr.2014.09.028.

[43] R.D. Gietz, R.H. Schiestl, High-efficiency yeast transformation using the LiAc/SS carrier DNA/PEG method, Nat. Protoc. 2 (2007) 31–34 https://doi.org/10.1038/nprot.2007.13.

[44] J. Soares, M. Espadinha, L. Raimundo, H. Ramos, A.S. Gomes, S. Gomes, J.B. Loureiro, A. Inga, F. Reis, C. Gomes, M.M.M. Santos, L. Saraiva, DIMP53-1: a novel small-molecule dual inhibitor of p53-MDM2/X interactions with multifunctional p53-dependent anticancer properties, Mol. Oncol. 11 (2017) 612–627 https://doi.org/10.1002/1878-0261.12051.

[45] B.X. Tan, C.J. Brown, F.J. Ferrer, T.Y. Yuen, S.T. Quah, B.H. Chan, A.E. Jansson, H.L. Teo, P. Nordlund, D.P. Lane, Assessing the Efficacy of Mdm2/Mdm4-Inhibiting Stapled Peptides Using Cellular Thermal Shift Assays, Sci. Rep. 5 (2015) 12116 https://doi.org/10.1038/srep12116.

[46] B.M. Gyori, G. Venkatachalam, P.S. Thiagarajan, D. Hsu, M.-V. Clement, OpenComet: an automated tool for comet assay image analysis, Redox Biol 2 (2014) 457–465 https://doi.org/10.1016/j.redox.2013.12.020.

[47] J. Schindelin, C.T. Rueden, M.C. Hiner, K.W. Eliceiri, The ImageJ ecosystem: An open platform for biomedical image analysis, Mol. Reprod. Dev. 82 (2015) 518–529 https://doi.org/10.1002/mrd.22489.

[48] T.-C. Chou, P. Talalay, Quantitative analysis of dose-effect relationships: the combined effects of multiple drugs or enzyme inhibitors, Adv. Enzym. Regul. 22 (1984) 27–55 https://doi.org/10.1016/0065-2571(84)90007-4.

[49] A.E. Vilgelm, M.K. Washington, J. Wei, H. Chen, V.S. Prassolov, A.I. Zaika, Interactions of the p53 protein family in cellular stress response in gastrointestinal tumors, Mol. Canc. Therapeut. 9 (2010) 693–705 https://doi.org/10.1158/1535-

7163.MCT-09-0912.
[50] E. Horvilleur, M. Bauer, D. Goldschneider, X. Mergui, A. de la Motte, J. Benard, S. Douc-Rasy, D. Cappellen, p73alpha isoforms drive opposite transcriptional and post-transcriptional regulation of MYCN expression in neuroblastoma cells, Nucleic Acids Res. 36 (2008) 4222–4232 https://doi.org/10.1093/nar/gkn394.
[51] T. Van Maerken, F. Speleman, J. Vermeulen, I.L. Lambertz, S. De Clercq, E. De Smet, N. Yigit, V. Coppens, J. Philippe, A. De Paepe, J.-C. Marine, J. Vandesompele, Small-molecule MDM2 antagonists as a new therapy concept for neuroblastoma, Cancer Res. 66 (2006) 9646–9655 https://doi.org/10.1158/0008-5472.CAN-06-0792.
[52] A.S. Gomes, P. Brandao, C.S.G. Fernandes, M.R.P.C. da Silva, M.E.P. de Sousa, M.M.d.M. Pinto, Drug-like Properties and ADME of Xanthone Derivatives: The Antechamber of Clinical Trials, Curr. Med. Chem. 23 (2016) 3654–3686 https://doi.org/10.2174/0929867323666160425113058.
[53] P.J. O'Brien, A.G. Siraki, N. Shangari, Aldehyde Sources, Metabolism, Molecular Toxicity Mechanisms, and Possible Effects on Human Health, Crit. Rev. Toxicol. 35 (2005) 609–662 https://doi.org/10.1080/10408440591002183.
[54] D. Goldschneider, E. Blanc, G. Raguenez, M. Barrois, A. Legrand, G. Le Roux, H. Haddada, J. Benard, S. Douc-Rasy, Differential response of p53 target genes to p73 overexpression in SH-SY5Y neuroblastoma cell line, J. Cell Sci. 117 (2004) 293–301 https://doi.org/10.1242/jcs.00834.
[55] M. Huang, W.A. Weiss, Neuroblastoma and MYCN, Cold Spring Harb. Perspect. Medicine 3 (2013) a014415 https://doi.org/10.1101/cshperspect.a014415.
[56] J.M. Maris, M.D. Hogarty, R. Bagatell, S.L. Cohn, Neuroblastoma, Lancet 369 (2007) 2106–2120 https://doi.org/10.1016/S0140-6736(07)60983-0.
[57] A. Nakagawara, M. Ohira, Comprehensive genomics linking between neural development and cancer: neuroblastoma as a model, Cancer Lett. 204 (2004) 213–224 https://doi.org/10.1016/S0304-3835(03)00457-9.
[58] V. De Laurenzi, G. Raschella, D. Barcaroli, M. Annicchiarico-Petruzzelli, M. Ranalli, M.V. Catani, B. Tanno, A. Costanzo, M. Levrero, G. Melino, Induction of neuronal differentiation by p73 in a neuroblastoma cell line, J. Biol. Chem. 275 (2000) 15226–15231 https://doi.org/10.1074/jbc.275.20.15226.
[59] K.K. Matthay, J.G. Villablanca, R.C. Seeger, D.O. Stram, R.E. Harris, N.K. Ramsay, P. Swift, H. Shimada, C.T. Black, G.M. Brodeur, R.B. Gerbing, C.P. Reynolds, Treatment of high-risk neuroblastoma with intensive chemotherapy, radiotherapy, autologous bone marrow transplantation, and 13-cis-retinoic acid. Children's Cancer Group, N. Eng. J. Medicine 341 (1999) 1165–1173 https://doi.org/10.1056/NEJM199910143411601.
[60] N.R. Pinto, M.A. Applebaum, S.L. Volchenboum, K.K. Matthay, W.B. London, P.F. Ambros, A. Nakagawara, F. Berthold, G. Schleiermacher, J.R. Park, D. Valteau-Couanet, A.D. Pearson, S.L. Cohn, Advances in Risk Classification and Treatment Strategies for Neuroblastoma, J. Clin. Oncol. 33 (2015) 3008–3017 https://doi.org/10.1200/JCO.2014.59.4648.
[61] E. Barbieri, P. Mehta, Z. Chen, L. Zhang, A. Slack, S. Berg, J.M. Shohet, MDM2 inhibition sensitizes neuroblastoma to chemotherapy-induced apoptotic cell death, Mol. Canc. Therapeut. 5 (2006) 2358–2365 https://doi.org/10.1158/1535-7163.MCT-06-0305.
[62] J. Cinatl, D. Speidel, I. Hardcastle, M. Michaelis, Resistance acquisition to MDM2 inhibitors, Biochem. Soc. Trans. 42 (2014) 752–757 https://doi.org/10.1042/BST20140035.